cite peer-reviewed, updated version:
Russell, R. P., Lara, M., "On the Design of an Enceladus Science Orbit," Acta Astronautica, Vol. 65, No. 1-2, 2009, pp. 27-39.

On the Design of an Enceladus Science Orbit*

Ryan P. Russell †
Georgia Institute of Technology, Atlanta, GA, 30332-0150

and

Martin Lara ‡
Real Observatorio de la Armada, 11110 San Fernando, Spain

Recent Cassini discoveries have quickly thrust Enceladus into the science spotlight. Unfortunately, the low Enceladus mass and its proximity to Saturn lead to extreme instabilities when considering typical near polar science orbits. Here we find that the usual doubly averaged techniques are invalid for realistic Enceladus orbits. Further, it is shown that a dependence on the low order averaging assumptions leads to overly conservative conclusions regarding stability boundaries. Instead, we rely on the results of global searches for periodic orbits in the unaveraged model and demonstrate long term stable orbits with altitudes near 200 km and inclinations approaching 65 degrees. Prior studies imply the maximum stable inclination is near 45 degrees.

Nomenclature

Symbol	***Description***
a, e, i, ω, Ω, υ	Classical orbital elements: semi-major axis, eccentricity, inclination, argument of periapse, longitude of ascending node, true anomaly
alt	altitude
b_1 , b_2	Stability indices
C	Jacobi integral of motion
r	Radius magnitude of the spacecraft position
M	Approximate number of Enceladus revolutions
N	Exact number of spacecraft revolutions
U	Nonspherical gravity potential
x, y, z, u, v, w	Rotating, Enceladus centered, body fixed state components
X,Y,Z,U,V,W	Nonrotating, Enceladus centered state components
Γ	Potential function
μ	Enceladus gravitational parameter
n	Enceladus mean motion

I. Introduction

The topic of science orbit design around planetary moons is broad and has been the subject of many important studies in recent years. See, for example, References [1-19]. In order to ensure global coverage, adequate surface mapping, and tidal bulge detection, science orbits are required to have high inclination, low altitude, and low eccentricity. Unfortunately, it is well known that most orbits about planetary satellites with these properties are dynamically unstable. At Europa (the subject of most recent applications), Jupiter's third body effects drive this

* Presented as Paper AIAA-2008-7072 at the AIAA/AAS Astrodynamics Specialist Conference, Honolulu, HI, August 20, 2008.
† Assistant Professor, Guggenheim School of Aerospace Engineering, 270 Ferst Drive, 404-385-3342, ryan.russell@gatech.edu, Member AIAA. *Formerly*: Jet Propulsion Laboratory, California Institute of Technology, 4800 Oak Grove Drive, Pasadena, CA 91109.
‡ Commander, Ephemerides section, mlara@roa.es. Member AIAA.

cite peer-reviewed, updated version:
Russell, R. P., Lara, M., "On the Design of an Enceladus Science Orbit," Acta Astronautica, Vol. 65, No. 1-2, 2009, pp. 27-39.

instability leading to ballistic orbits that impact on the order of 20→40 days for arbitrary orbits. At Enceladus, its low mass and proximity to Saturn reduces the characteristic impact times to 1→3 days (for low altitude polar orbits) [10]. The judicious use of unstable "frozen" polar orbits such as those studied in [6, 8] indeed can increase the characteristic impact times at Enceladus to 1→2 weeks. Despite the improvement compared to a just few days, even the frozen polar orbits remain too risky for serious consideration. Thus emerges the primary objective of the current study: *Identify long- term stable, low altitude Enceladus science orbits with maximized inclinations.*

The first order dynamics of orbiters in the vicinity of planetary moon satellites are captured nicely thru averaging techniques that reduce the dimension of the problem from six to effectively three enabling a thorough characterization of possible motion. For details on studies that rely on averaging see [2,4,8,9,10]. A second general technique for analyzing motion near planetary moons involves the search and characterization of periodic orbits in unaveraged models. See [4,5,6,11,12,13,14,16,17] for details. The important consideration of nonconservative perturbations (the realistic ephemeris for example) and force model uncertainties also play key roles in the detailed stability analysis and design of science orbits at planetary moons. While Refs. [5,6,11,14,15] represent progress in this area, more detailed analyses regarding the transition from simplified dynamics to ephemeris models is a ripe area of future research.

The current study is based primarily on the results of [2,13,14,18]. The doubly averaged third body problem from [2] is applied at Enceladus in [18] to assess possible orbiter motion in a global context. The results of [18] indicate that the radius of Enceladus fills a substantial fraction of the region around Enceladus where the doubly averaged system is valid. Therefore, when considering only nonimpact orbits, we conclude that the typical first order doubly averaged system is only marginally valid at Enceladus even for very low altitude orbits. However, we note also that the region of validity for the averaging models has fuzzy boundaries in reality. Understanding the doubly averaged system does provide some insight and confidence of a global perspective of potential qualitative motion. Although we leave a detailed investigation to future works, Enceladus is an excellent candidate application for higher order averaging of the Hill's model where the long-term dynamics are described more adequately [19]. A cursory investigation based on the results of [19] shows stable inclinations for low eccentricity, ~250 km orbits at Enceladus exist up to 54 degrees, a significant improvement to the first-order predictions.

In this paper, we resort our focus away from averaging techniques and instead to the computation and analysis of periodic orbits in unaveraged models. The global search for stable periodic orbits archived in [13] is scalable for all small planetary moons and gives rise to a second global picture of possible orbits around Enceladus. The dynamical model in [13] is the unaveraged Restricted Three Body Problem (RTBP) and has a much larger region of validity compared to the doubly averaged problem. It does not however include any nonspherical moon gravity terms. However, the global grid search is sufficient for identifying the most promising (stable and highly inclined) candidate orbits for a more detailed local analysis using a higher fidelity model.

Provided the initial guesses from the grid search from [13], local periodic orbit searches are performed in the Saturn-Enceladus Hill's model superimposed on a J_2 plus J_3 plus C_{22} Enceladus spherical harmonic gravity field. The Hill's third body potential and the nonspherical two body potential are both time invariant; therefore, an abundance of periodic orbits exists, computational searches are relatively fast, and stability information accompanies the solutions at no extra cost. Natural families of solutions are then generated based on predictor corrector procedures that originate with the first converged solution. The families are convenient for general orbit design purposes because they can generally be parameterized as continuous functions of mean inclination. We note that for this study, the periodic orbits and families of orbits were found and verified using two independent software suites. The algorithms and concepts are explained and demonstrated in [6,11,14,16,20].

Finally, after evaluating a host of potential families for stability and maximized inclinations, we demonstrate example families that enjoy stable orbits with inclinations as high as 67 degrees. In a full ephemeris *n* body model simulation, an example solution reveals a maximum inclination of 64 degrees and is long term stable for at least 6 months. This finding is significant because it is conservatively fifteen degrees greater in inclination than that implied in the Enceladus 2007 Flagship Report to NASA Headquarters (page 79/148 Fig. 3-3-3-7) [§] as being the maximum attainable stable inclination.

[§] http://www.lpi.usra.edu/opag/announcements.html [cited June 3 2008]
http://www.lpi.usra.edu/opag/Enceladus_Public_Report.pdf [cited June 3 2008]

cite peer-reviewed, updated version:
Russell, R. P., Lara, M., "On the Design of an Enceladus Science Orbit," Acta Astronautica, Vol. 65, No. 1-2, 2009, pp. 27-39.

II. Models and Parameters

The equations of motion for the Hill's plus nonspherical gravity model are given in Eq. (1). For details on the Hill's approximation to the Restricted Three Body Problem, see for example, [21].

$$\begin{aligned} \ddot{x} &= 2nv + \partial\Gamma/\partial x \\ \ddot{y} &= -2nu + \partial\Gamma/\partial y \\ \ddot{z} &= \partial\Gamma/\partial z \end{aligned} \tag{1}$$

The potential function, Γ, is introduced in Eq. (2) where U is the contribution due to the nonspherical moon, and it is expressed via the standard spherical harmonic expansion [22]. Typically, canonical units (LU and TU) are derived based on normalizing the moon mean motion and gravitational parameter, n and μ respectively, to unity. Figure 1 illustrates the geometry. Note that the Enceladus body fixed frame is conveniently static in the Hill's rotating frame because the moon rotation rate is synchronously locked with the orbital mean motion.

$$\begin{aligned} \Gamma &= \frac{1}{2}n^2\left(3x^2 - z^2\right) + \mu/r + U \\ r &= \sqrt{x^2 + y^2 + z^2} \end{aligned} \tag{2}$$

The system is Hamiltonian and admits C, an integral of motion given in Eq. (3) that is analogous to the Jacobi constant.

$$C = 2\Gamma - \left(u^2 + v^2 + w^2\right) \tag{3}$$

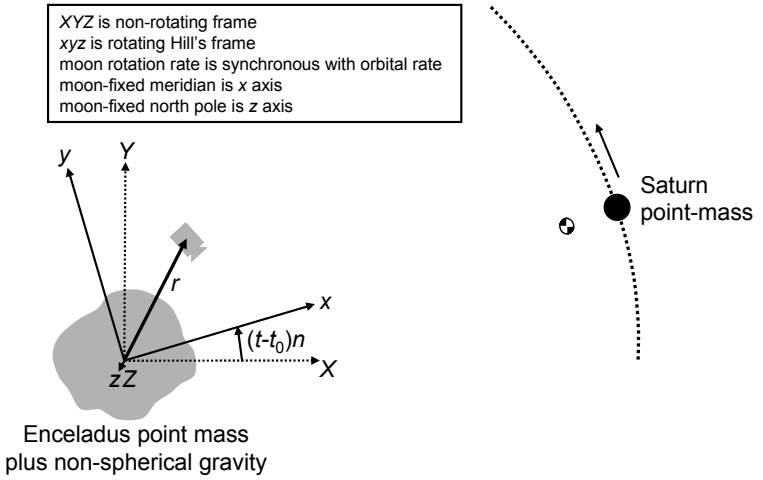

Figure 1: Hill's model plus nonspherical potential model

The important dynamic parameters used in this study are given in Table 1. The stated gravity field terms are normalized and arbitrarily chosen within the expected range.[**] Note that the Enceladus proximity to Saturn and associated fast spin rate leads to an expected J_2 value approximately an order of magnitude larger than Europa. Therefore, the J_2 and C_{22} are expected to play significant roles. We also note that the third body perturbations are similarly larger at Enceladus when compared to Europa. Therefore, despite the significant nonspherical gravity, the third body perturbations remain dominant. The "hot spot" on the south polar region of Enceladus and preliminary estimates of different north and south pole radii likely reflect a nonnegligible negative J_3 value [23,24]. For lack of a published estimate, the J_3 value given in Table 1 is chosen to sample potential effects.

[**] Estimates for the dominant gravity field terms are based on personal communication with Julie C. Castillo (jccastil@mail.jpl.nasa.gov). The unnormalized J_2 is expected to be in the range of 0.004 to 0.008 and the hydrostatic equilibrium assumption ($C_{22} = 3\ J_2\ /10$, unnormalized; or $C_{22} \sim J_2$, normalized) gives an expected unnormalized C_{22} range of 0.0012 to 0.0024.

cite peer-reviewed, updated version:
Russell, R. P., Lara, M., "On the Design of an Enceladus Science Orbit," Acta Astronautica, Vol. 65, No. 1-2, 2009, pp. 27-39.

Table 1. Enceladus and Saturn Parameters

Parameter	*Value*
Enceladus gravitational parameter (μ)	7.209544428892310 km^3/s^2
Saturn gravitational parameter	3,7940,000.0 km^3/s^2
Mass ratio (derived)	1.900248565867070E-07
System Rotation Rate (ω, derived)	5.303637005052082E-005
Enceladus mean radius	256.3 km
Enceladus normalized J_2	0.0025
Enceladus normalized J_3	-0.00001
Enceladus normalized C_{22}	0.0025
Saturn-Enceladus distance	238,040.0 km
Hill's model length unit (LU derived)	1368.52713426300 km
Hill's model time unit (TU derived)	18854.9857210709 s
Approximate Saturn-Enceladus Lagrange point distance (derived)	~950 km

While the inclusion of higher order gravity field terms is a second order effect assuming Enceladus is close to hydrostatic equilibrium, the periodic orbit approach implemented in this study is amenable to including these higher order terms, even in the case of a highly irregular shaped body [14]. The rapid identification of the long life periodic orbits in a full gravity field is well suited for future Monte-Carlo analyses that will certainly be required to investigate gravity field sensitivities. Note that the largely analytical averaging techniques may prove difficult if not impossible to include higher order terms.

Selected ephemeris propagations are carried out to demonstrate robustness of the simplified model solutions to perturbations associated with realistic force models. The ephemeris states of the planets, the Sun, Titan, and Enceladus are based on publicly available[*] data from the Jet Propulsion Laboratory. The poles and prime meridians for Saturn and Enceladus are based on the most recent data from the IAU Working Group on Cartographic Coordinates and Rotational Elements of the Planets and Satellites [25].

III. Typical Enceladus Orbits

The doubly averaged third body problem is discussed in detail in [2], for example, where the third body potential is averaged twice: once over one spacecraft orbit and once over one system orbit. It is well known that low eccentricity orbits with inclinations greater than the critical value (39.6^o), global motion is restricted to orbits that circulate or librate in argument of periapse and repeatedly cycle between a low eccentricity and some maximum value. An orbiter will impact the surface of a planetary moon in short order unless the maximum eccentricity associated with its librating or circulating cycle is sufficiently small such that the periapse is larger than the moon radius. In order to avoid impacts at top of the eccentricity cycle, a mission designer must therefore choose a sufficiently high value for the semi-major axis [18]. In the doubly averaged system, the semi-major axis secular rate is zero and therefore only scales the time evolution of the reduced variable set $\{e, i, \omega\}$. However, we are limited in the selection of a large semi-major axis due to the basic assumptions regarding the doubly averaged model that assume the spacecraft period is much smaller than the system period.[††] The typical order of magnitude difference [10] in the orbiter and system period in the case of Enceladus leads to a maximum semi-major axis near 295 km. Considering the radius of Enceladus is 256 km, there is little margin for eccentricity (or navigation error). Even if the orbiter period is doubled (increased to one fifth that of the system period: a more clear violation of the averaging assumptions), the maximum orbiter semi-major axis becomes 468 km. This allows for a maximum eccentricity of 0.25 if a 100 km minimum altitude is enforced. Accordingly, only inclinations below 42^o degrees will find acceptable maximum eccentricity [18].

[*] URL: http://naif.jpl.nasa.gov/naif/spiceconcept.html [cited 16 Jun 2008].
URL: ftp://naif.jpl.nasa.gov/pub/naif/generic_kernels/spk/planets/a_old_versions/de414.bsp [cited 16 Jun 2008].
URL: ftp://naif.jpl.nasa.gov/pub/naif/generic_kernels/spk/satellites/a_old_versions/sat242.bsp [cited 16 Jun 2008].
URL: ftp://naif.jpl.nasa.gov/pub/naif/generic_kernels/pck/pck00008.tpc [cited 16 Jun 2008].

[††] Note that doubly averaged model validity is indirectly related to semi-major axis.

cite peer-reviewed, updated version:
Russell, R. P., Lara, M., "On the Design of an Enceladus Science Orbit," Acta Astronautica, Vol. 65, No. 1-2, 2009, pp. 27-39.

The doubly averaged model is found therefore to be only marginally valid at Enceladus because the period of any realistic orbiter (minimum altitudes of ~100 km) is arguably too large to justify the averaging assumptions. While the precise boundaries of model validity are quantitatively debatable [10,18], comparisons between the averaged and unaveraged models are easy to implement for specific cases. Numerical simulations performed in the unaveraged model starting with near circular 200 km altitude orbits show consistent results with the averaged model analysis (even with the averaging assumptions being pushed perhaps beyond their valid limits). The conclusion that *arbitrary* initial conditions for near circular 200 km altitude orbits with inclinations above 45^o generally lead to impacts is consistent with the findings in the Enceladus 2007 Flagship Report[§]. In the following section, we will investigate *nonarbitrary* intitial conditions in an effort to seek stable orbits with greater inclinations.

IV. Periodic Enceladus Science Orbits in the Unaveraged Model

In order to more accurately characterize the motion at Enceladus for distances beyond the region of validity for the doubly averaged problem, we rely on a global view of the periodic orbits and families in the unaveraged equations [5,12,13]. Of the most promising results in [5,12,13] was the observation and characterization of a large class of stable yet highly inclined direct orbits. This class of orbits exists in the vicinity near 3/5 of the Lagrange point distance and represents the largest inclinations of the stable orbits found in the global search documented in [13]. Further, most of the orbits have small e and variations in e as compared with many other three body orbits at those distances. Orbits of this nature exist beyond the region of validity for the doubly averaged dynamics. At Europa, these orbits have high altitudes with semi-major axes near ~8000 km. An example such highly inclined, near circular orbit at Europa is given in Figure 2.

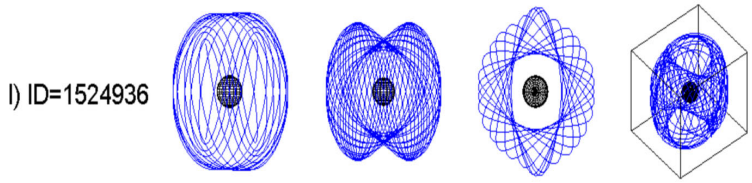

Figure 2: Four views of an example highly inclined stable orbit at Europa (picture taken from [13], ID=1524936)

Serendipitously when the orbit from Figure 2 is scaled to the Enceladus distance and times, the average semi-major axis is ~550 km, very near what scientists and mission planners would desire for an Enceladus orbiter. Therefore, we proceed by seeking to find orbits such as these in the Saturn-Enceladus system. Using the initial conditions from the orbit in Figure 2 (scaled to Enceladus), the differential corrector software described in the introduction easily converges to a solution in the Saturn-Enceladus system when Enceladus is treated as a point mass. The higher fidelity solution is then found including the large nonspherical gravity terms given in Table 1 using a continuation method. Provided a single converged periodic orbit, the natural family of similar orbits can then be found by targeting neighboring Jacobi constants. The effect of changing the Jacobi constant on this family in the vicinity of the orbit of interest is small changes in average inclination.

As an example we seek periodic orbits near Enceladus that belong to the 8:35 class of families, noting that the spacecraft makes 35 revolutions while Enceladus makes $8+\Delta\Omega$ revolutions prior to closing the periodic orbit in the body fixed frame. The ratio of the two integers can be adjusted in order to change the average semi-major axis [14]. The 8:35 class of families is selected to provide orbits with average semi-major axes near 500 km and to remain consistent with the geometry of the stable highly inclined orbits found in [13]. Figure 3 shows the evolution of an example family for a course Jacobi constant resolution. The inclination-stability diagram (dotted b_1 and b_2 curves) is combined with the inclination-eccentricity diagram (non-vertical full line). The vertical line and intersecting off-colored dots denote a single example solution at 60.3^o for later evaluation. We see that there exist stable periodic orbits in the range $57.5^o < i < 61.4^o$ deg, with one stability index bounded by the critical values ±2 while the other is always very close to +2. The more promising solutions for mission design purposes are the stable orbits with the higher inclinations.

cite peer-reviewed, updated version:
Russell, R. P., Lara, M., "On the Design of an Enceladus Science Orbit," Acta Astronautica, Vol. 65, No. 1-2, 2009, pp. 27-39.

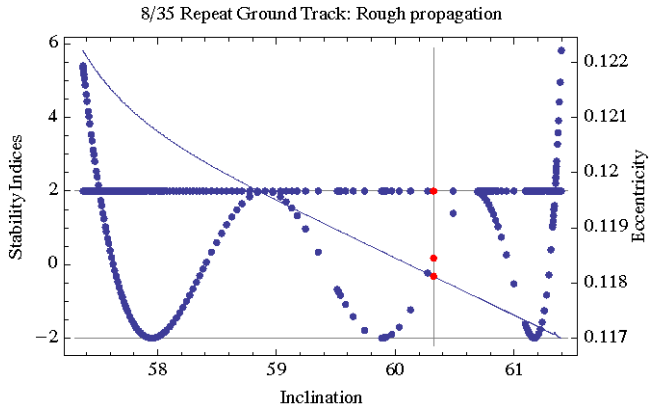

Figure 3: Course resolution 8:35 families of science orbits at Enceladus (see text for explanation).

A finer resolution analysis of the family behavior near 61° shows that Figure 3 is in fact made of different families, due to the rapid occurrence of bifurcations and reflections in the Jacobi constant value (generating parameter for the family of solutions). Accordingly, the Appendix gives detailed initial conditions for three different stable orbits with the same averaged inclination (61.3°) and similar other orbital elements. Note that the complex structure of intersecting families is typical for long period, multi-revolution periodic orbits.

To demonstrate the properties of a particular orbit, we select one of the stable orbits towards the middle of stability region from Figure 3 (corresponding to the vertical line). Figure 4 - Figure 6 show characteristics of an example solution propagated for one period. The three body nature of the orbit is appreciated in the large variations seen in the osculating orbital elements shown in Figure 4. The orbit has altitudes ranging from 190→290 km, eccentricities ranging from 0.06 to 0.19, and inclinations ranging from 55° to 64°. The argument of periapse is clearly of the circulating nature [18] as it cycles exactly 19 times in the brief ~10 day period. Note the figure eight pattern of the close approach locations on the right side of Figure 5. Figure 6 illustrates the exact repeat pattern of the eccentricity vector over the course of 1 period.

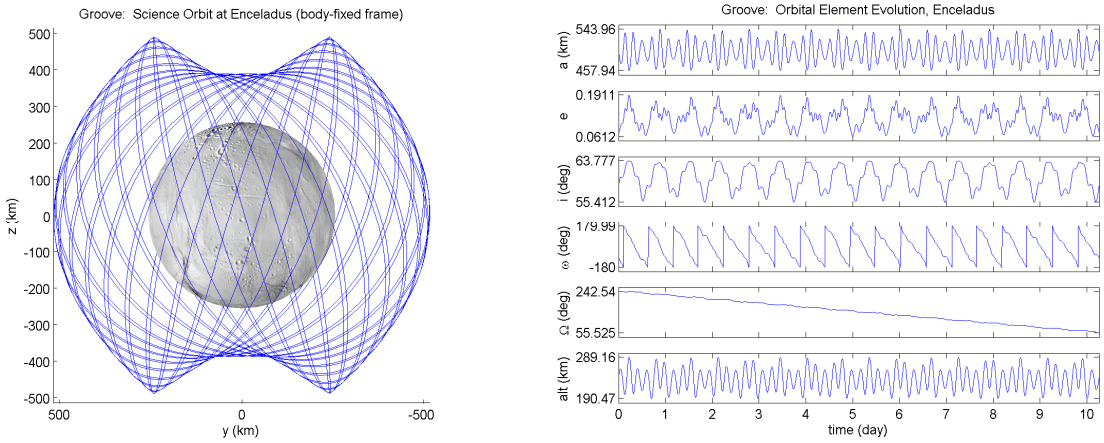

Figure 4: One period of example 8:35 science orbit: trajectory (left) and orbital elements (right)

cite peer-reviewed, updated version:
Russell, R. P., Lara, M., "On the Design of an Enceladus Science Orbit," Acta Astronautica, Vol. 65, No. 1-2, 2009, pp. 27-39.

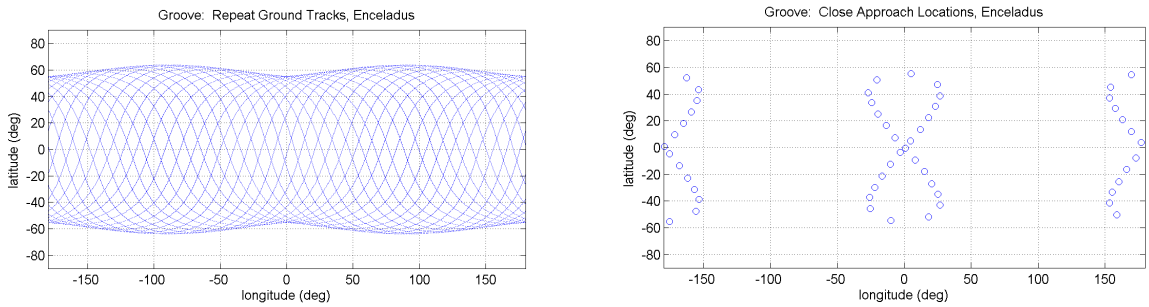

Figure 5: One period of example 8:35 science orbit: full ground tracks (left) and close approaches (right)

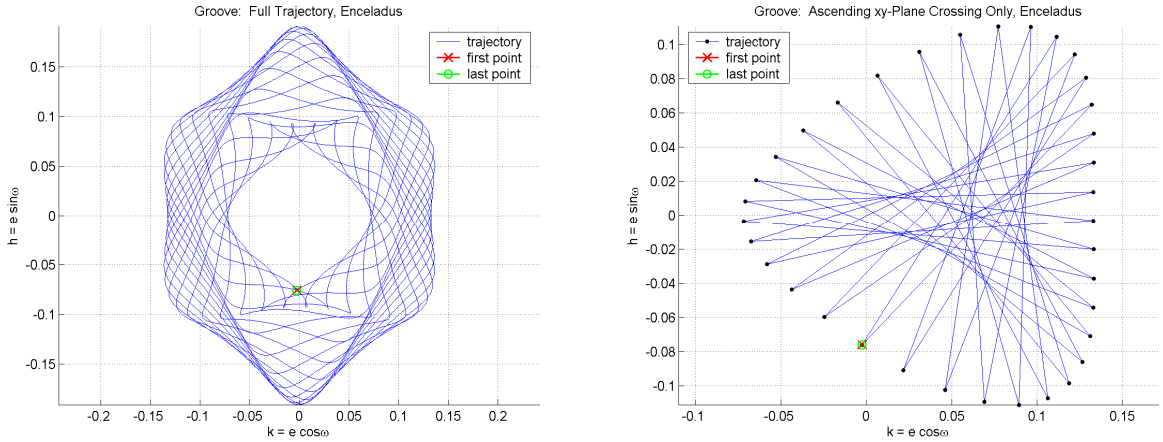

Figure 6: One period of example 8:35 science orbit: full (left) and plane crossings (right) eccentricity vector repeat paths

It is emphasized that the 8:35 class of families shown in Figure 3 is simply one example with an *M:N* ratio that is favorable for Enceladus science orbits. To illustrate an alternative ratio (9:35), we show in Figure 7 a similar family of orbits with a slightly larger average altitudes. The vertical line and intersecting off-colored dots denote a single example solution at 62.53°. The semi-major axes of the members of the 9:35 class of families are close to the 550 km value that is predicted to have stable orbits with the largest possible inclinations. Accordingly, Figure 7 shows a general stable region of orbits with average inclinations between 62.4° and 63°. Again, a finer resolution analysis reveals that Figure 7 is made of different families. The initial conditions of two different stable orbits with the similar averaged orbital elements are given in the Appendix.

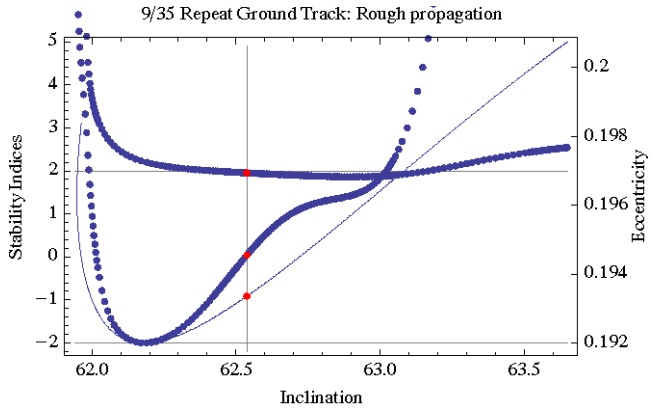

Figure 7: Course resolution 9:35 families of science orbits at Enceladus (see text for explanation).

An example stable member of the family from Figure 7 (corresponding to the vertical line) is illustrated in Figure 8. Note the orbit is linearly stable and achieves remarkably high instantaneous inclinations of nearly 67°. Table 2 gives the initial conditions for the example orbits from Figure 4 - Figure 6 and Figure 8.

Because the searches in [12, 13] were global in nature, we have confidence that the example families presented in Figure 3 and Figure 7 are at or near the most favorable possible solutions in terms of stability, altitudes, and inclinations. We should also note that in the vicinity of half the Lagrange point distance, the near circular direct families ($i < 90^o$) enjoy stability at inclinations slightly closer to polar than in comparison the retrograde families ($i > 90^o$) as illustrated in Figure 10 of [12]. Therefore, retrograde inclinations are not considered in this study.

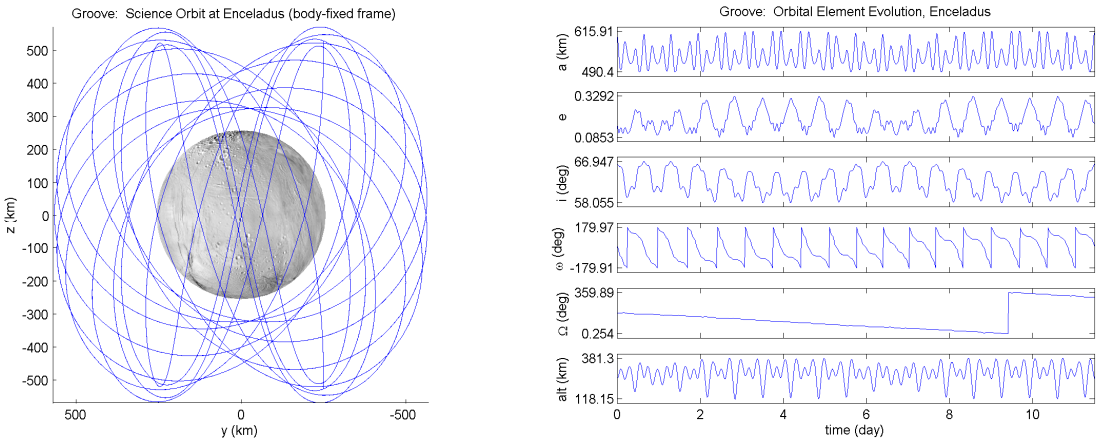

Figure 8: One period of example 9:35 science orbit: trajectory (left) and orbital elements (right)

cite peer-reviewed, updated version:
Russell, R. P., Lara, M., "On the Design of an Enceladus Science Orbit," Acta Astronautica, Vol. 65, No. 1-2, 2009, pp. 27-39.

Table 2. Example stable orbit data*

Property	Units	8:35 orbit	9:35 orbit
x_0	km	-0.2355272394516388E+03	-0.5082596695187572E+03
y_0	km	-0.4377725059013570E+03	-0.1800936879269212E+02
z_0	km	0	0
u_0	km/s	0.5065296483365822E-01	0.7394978609598108E-02
v_0	km/s	-0.3764519699459160E-01	-0.5133316669397093E-01
w_0	km/s	0.1028014839043201E+00	0.1174895301192797E+00
a_0	km	0.4987636181497566E+03	0.6079812097695036E+03
e_0	-	0.7594742316109369E-01	0.1690071708641842E+00
i_0	deg	0.5872499513454099E+02	0.6630468636656518E+02
ω_0	deg	-0.9185596836014398E+02	0.1736359903905670E+02
Ω_0	deg	0.2417191769293457E+03	0.1820293353333430E+03
υ_0	deg	$-\omega_0$	$-\omega_0$
T	day	0.1026020511894865E+02	0.1148182606420868E+02
avg. i	deg	60.3	62.5

*Initial conditions given in nonrotating frame aligned with the IAU defined Enceladus body fixed frame at epoch.

V. Long Term n Body Propagations

The stable solutions highlighted in this study are considered linearly stable in the conservative force model including the Hill third body perturbation and the nonspherical gravity terms from Table 1. The radius of the stability regions around the stable orbits in the presence of numerical and other perturbations is unclear. Methods using Fast Lyapynov Indicators (FLIs) are useful for estimating stability region radii [5,15]. While no such method has been applied in the current study, it is an important area of future work.

Ephemeris *n* body propagations are a simpler, cruder approach to measuring stability radii or robustness of a particular solution to nontrivial perturbations. Therefore we proceed by propagating the two example orbits in ephemeris simulations involving two body gravity from the Sun, Jupiter, Saturn, Titan and Enceladus; and oblateness effects from Saturn and Enceladus. By specifying the initial conditions in body fixed frames at epoch given in Table 2, propagations beginning at arbitrary epochs have the effect of sampling uncertainties in the force model. If a particular orbit maintains its basic characteristics without impacting or escaping for 180 days (600+ revolutions around Enceladus) for 10 arbitrarily chosen epochs, it is considered long term stable.

Figure 9 and Figure 10 show characteristics of the 8:35 example orbit ephemeris propagation. The epoch is arbitrarily chosen as Jan. 1, 2028 (Julian Date = 2461772.0). This orbit is deemed long term stable as each of the 10 different epochs led to orbital lifetimes of at least 180 days. By comparing the eccentricity vector path and the close approach locations of the simplified model equivalents in Figure 5 and Figure 6, it is clear that basic orbital characteristics are maintained during the long term propagation. It should be noted that the example orbits were taken from the middle of the stability regions in Figure 3 and Figure 7 to avoid the stability boundaries that could lead to less robust solutions in the realistic force models.

Despite being stable in the conservative model, the highly inclined 9:35 orbit depicted in Figure 8 failed to achieve long term stability in the ephemeris propagations. In most cases, the orbit impacted or escaped after approximately 10 days. As the example 9:35 orbit is very close to the predicted maximum possible stable inclination in the conservative model, it is not surprising that the orbit fails the stability test using ephemeris perturbations. Based on this preliminary analysis, the 8:35 orbit is considered long term stable, but likely is close to the realistic perturbation stability boundary in terms of inclination.

A brief analysis was performed to spot check the sensitivity of the long term propagation to the nonspherical gravity of Enceladus. The same stability test of applying ten arbitrary epochs led to similar long term stable results using only a point mass term for Enceladus. While this result is promising and likely due to the large altitudes when compared to the Enceladus radius, considerable future work is required to understand the nonspherical gravity field implications.

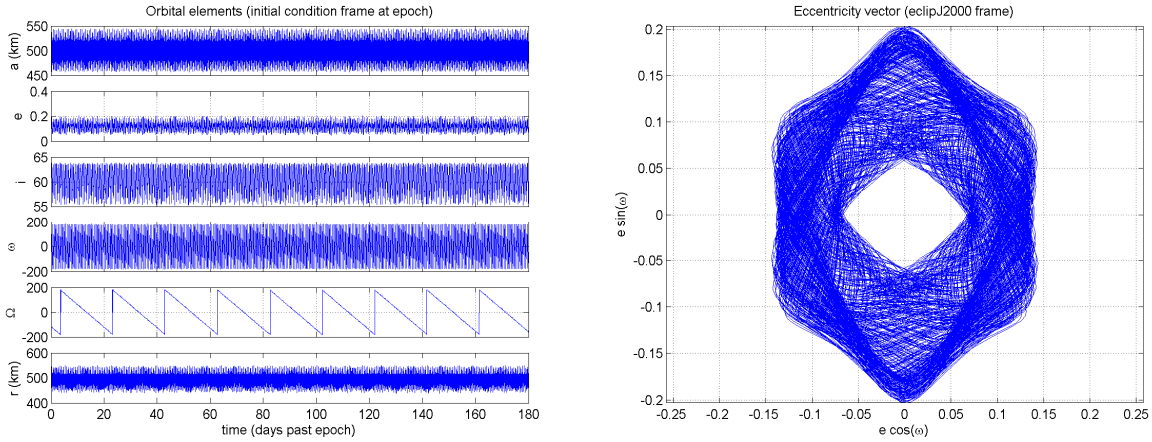

Figure 9: Long term n body ephemeris propagation of example 8:35 science orbit: orbital elements evolution (left) and full eccentricity vector repeat path (right)

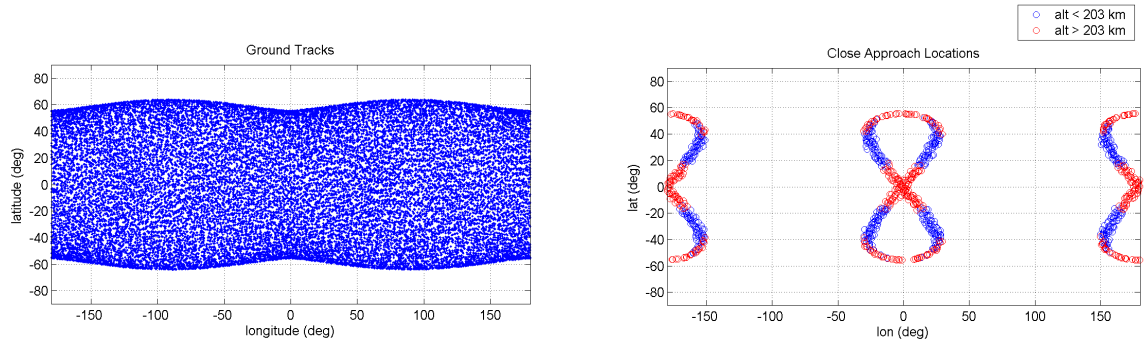

Figure 10: Long term n body ephemeris propagation of example 8:35 science orbit: full ground tracks (left) and close approaches (right)

VI. Conclusion

A 200 km altitude science orbit at Enceladus is found to exist beyond the formal region of validity for the doubly averaged dynamics. While the doubly averaged system provides general insight to the third body problem, we rely mainly on the unaveraged system for characterizing global motion for potential Enceladus orbiters. The results of prior global grid searches and characterizations of families of periodic orbits in the unaveraged problem point us towards a class of highly inclined candidates for stable science orbits at Enceladus. Finally, a largely nonspherical gravity field is incorporated and continuous families of stable periodic orbits are identified and analyzed. Fine resolution analyses of the multi-revolution orbits reveal complex structures of bifurcating families. Representative solutions with desired science orbit characteristics are demonstrated as long term stable in a full ephemeris model.

The example highly inclined, long term stable orbit presented is believed to be near the maximum feasible inclination for stable low altitude orbits around Enceladus. This orbit has inclinations conservatively fifteen degrees higher than the maximum stable inclination at Enceladus predicted from the averaged dynamics and commonly accepted in the mission design community. The high altitudes compared to the body radius makes both poles viewable (including the "Tiger Stripes" near the southern pole) at near nadir pointing angles. The low eccentricities and near maximum achievable inclinations are suitable for science and communication purposes. The feasibility of long term, stable, high inclination orbits with polar visibility strengthens an already compelling argument to send a robotic orbiter to Enceladus.

cite peer-reviewed, updated version:
Russell, R. P., Lara, M., "On the Design of an Enceladus Science Orbit," Acta Astronautica, Vol. 65, No. 1-2, 2009, pp. 27-39.

Appendix

Table 3 and Table 4 give initial conditions in the rotating frame for example solutions revealed in the fine resolution analyses.

Table 3. Example initial conditions for 8:35 class

Property	Units	Orbit 1	Orbit 2	Orbit 3
x_0	km	0.1070240877013849E+03	0.4702710649001015E+03	-0.4709341748219429E+03
y_0	km	-0.5047527521556340E+03	0.4961398579457529E+01	0.2005016972812331E+02
z_0	km	0	0	0
u_0	km/s	0.3184065881751783E-01	0.4051686583303566E-02	-0.3988848384301891E-03
v_0	km/s	-0.6892035591461924E-04	0.3187660576447689E-01	-0.3186324972256872E-01
w_0	km/s	0.9792816171758140E-01	0.1188649418270250E+00	0.1187927410507614E+00
T	s	0.8859200773556026E+06	0.8853012736250127E+06	0.8880418913591516E+06
avg. a	km	497.234	496.981	498.101
avg. e	-	0.123103	0.125187	0.117230
avg. i	deg	61.3097	61.3101	61.3096
min r	km	420.978	413.117	449.010
max r	km	560.702	566.700	545.359

Table 4. Example initial conditions for 9:35 class

Property	Units	Orbit 1	Orbit 2
x_0	km	-0.3628578738543753E+03	-0.5092932103616286E+03
y_0	km	0.3466896463522740E+03	0.5196587731438462E+01
z_0	km	0	0
u_0	km/s	-0.1355838999154557E-01	0.3088464696888617E-02
v_0	km/s	-0.2754409761374015E-01	-0.2181039809713168E-01
w_0	km/s	-0.1131541724302042E+00	0.1181095845649803E+00
T	s	0.9896641998233017E+06	0.9896558154860166E+06
avg. a	km	540.674	540.670
avg. e	-	0.196533	0.196541
avg. i	deg	63.0298	63.0299
min r	km	344.792	344.521
max r	km	653.819	653.970

Acknowledgments

Part of this work has been performed at the Jet Propulsion Laboratory, California Institute of Technology, under a contract with the National Aeronautics and Space Administration. R.P.R. thanks Nathan Strange for help with initiating the project and ongoing consultation. A special thanks is owed to Kim Reh, Tom Spilker, John Elliot, and Jim Cutts for their interest and support. M.L. acknowledges partial support from the Spanish Government (project numbers ESP 2007-64068).

References

[1] Aiello, J., "Numerical Investigation of Mapping Orbits about Jupiter's Icy Moons," paper AAS 2005-377, presented at the 2005 Astrodynamics Specialists Conference, Lake Tahoe, California, August 2005.

[2] Broucke, R., "Long-Term Third-Body Effects via Double Averaging," *Journal of Guidance, Control and Dynamics*, Vol. 26, No. 1, 2003, pp. 27–32.

[3] Johannesen, J.R., and D'Amario, L.A., "Europa Orbiter Mission Trajectory Design," paper AAS 99–360, presented at the 1999 AAS/AIAA Astrodynamics Specialist Conference, Girdwood, Alaska, August 1999.

[4] Lara, M., and San-Juan, J.F., "Dynamic Behavior of an Orbiter Around Europa," *Journal of Guidance, Control and Dynamics*, Vol. 28, No. 2, 2005, pp. 291–297.

[5] Lara, M., Russell, R., and Villac, B., "On Parking Solutions Around Europa" paper AAS 2005-384, presented at the 2005 AAS/AIAA Astrodynamics Specialist Conference, Lake Tahoe, California, August 2005.

[6] Lara, M., Russell, R.P., "On the Design of a Science Orbit about Europa," paper AAS 06-168, presented at the 16th AAS/AIAA Space Flight Mechanics Conference, Tampa, Florida, January 22-26, 2006.

[7] Lara, M., San-Juan, J.F., and Ferrer, S., "Secular Motion around TriAxial, Synchronously Orbiting, Planetary Satellites: Application to Europa," *Chaos: An Interdisciplinary Journal of Nonlinear Science*, Vol. 15, No. 4, 2005, pp. 1–13.

[8] Paskowitz, M.E. and Scheeres, D.J., "Orbit Mechanics about Planetary Satellites," paper AAS 04-244, presented at the Space Flight Mechanics Meeting, Maui, Hawaii, February 2004.

[9] Paskowitz, M.E., and Scheeres, D.J., "Transient Behavior of Planetary Satellites Including Higher Order Gravity Fields," paper AAS 2005-358, presented at the 2005 Astrodynamics Specialists Conference, Lake Tahoe, California, August 2005.

[10] Scheeres, D.J., Guman, M.D., and Villac, B.F., "Stability Analysis of Planetary Satellite Orbiters: Application to the Europa Orbiter," *Journal of Guidance, Control, and Dynamics*, Vol. 24, No. 4, 2001, pp. 778–787.

[11] Lara, M., Russell, R. P., "On the Computation of a Science Orbit about Europa," *Journal of Guidance, Control, and Dynamics*. Vol. 30, No. 1, 2007, pp. 259-263.

[12] Lara, M., Russell, R.P., Villac, B. "Classification of the Distant Stability Regions at Europa," *Journal of Guidance, Control, and Dynamics*, Vol. 30, No. 2, 2007, pp. 409-418.

[13] Russell, R. P., "Global Search for Planar and Three-dimensional Periodic Orbits Near Europa," *Journal of the Astronautical Sciences*. Vol. 54, No. 2, 2006, pp. 199-226.

[14] Russell, R. P., Lara, M., "Long-Life Lunar Repeat Ground Track Orbits," *Journal of Guidance, Control, and Dynamics*, Vol. 30, No. 4, 2007, pp. 982-993.

[15] Lara, M., Russell, R.P., Villac, B. "Fast estimation of stable regions in real models," *Meccanica*, Springer, 2007, DOI 10.1007/s11012-007-9060-z.

[16] Lara, M., "Searching for Repeating Ground Track Orbits: A Systematic Approach," *Journal of the Astronautical Sciences*, Vol. 47, 1999, pp. 177–188.

[17] Lara, M., "Repeat Ground Track Orbits of the Earth Tesseral Problem as Bifurcations of the Equatorial Family of Periodic Orbits," *Celestial Mechanics and Dynamical Astronomy*, Vol. 86, No. 2, 2003, pp 143-162.

[18] Russell, R. P., Brinckerhoff, A.T., "Elliptic Orbits around Planetary Moons," Paper AAS 08-181, AAS/AIAA Space Flight Mechanics Meeting, Galveston, TX, Jan 2008.

[19] Lara, M., Palacián, J.F., "Hill Problem Analytical Theory to the Order Four. Application to the Computation of Frozen Orbits Around Planetary Satellites," Proceedings of the 20th International Symposium on Space Flight Dynamics, Annapolis, Maryland, September 24-28, 2007. reference number NASA/CP-2007-214158.

[20] Lara, M., Pel´aez, J., "On the Numerical Continuation of Periodic Orbits: An Intrinsic, 3-Dimensional, Differential, Predictor–Corrector Algorithm," *Astronomy and Astrophysics*, Vol. 389, Feb. 2002, pp. 692-701.

[21] Szebehely, V., Theory of Orbits. *The Restricted Problem of Three Bodies*, Academic Press, New York, 1967. pp. 602-629.

[22] Tapley, B.D., Schutz, B.E., Born, G.H., *Statistical Orbit Determination*, Elsevier Academic Press, Burlington, MA, 2004. Sec. 2.3.

[23] Hansen, C.J., L. Esposito, A. I. F. Stewart, J. Colwell, A. Hendrix, W. Pryor, D. Shemansky, R. West, "Enceladus' Water Vapor Plume", *Science,* 10 March 2006, Vo. 311, No. 5766, pp. 1422 – 1425, DOI: 10.1126/science.1121254.

[24] Porco, C.C., Helfenstein, P., Thomas, P.C., Ingersoll, A.P., Wisdom, J., West, R., Neukum, G., Denk, T., Wagner, Roatsch, T., Kieffer, S., Turtle, E., McEwen, A., Johnson, T.V., Rathbun, J., Veverka, J., Wilson, D., Perry, J. Spitale, J., Brahic, A., Burns, J. A., DelGenio, A.D., Dones, L., Murray, C.D., Squyres, S. "Cassini Observes the Active South Pole of Enceladus", *Science,* 10 March 2006, Vo. 311, No. 5766, pp. 1393 – 1401, DOI: 10.1126/science.1123013.

[25] Seidelmann, P.K., Abalakin, V.K., Bursa, M., Davies, M.E., Bergh, C. de, Lieske, J.H., Oberst, J., Simon, J.L., Standish, E.M., Stooke, P., Thomas, P.C., "Report of the IAU/IAG Working Group on Cartographic Coordinates and Rotational Elements of the Planets and Satellites: 2000," Celestial Mechanics and Dynamical Astronomy, Vol. 82, Issue 1, 2002, pp. 83–111.